NASA Electric Aircraft Testbed (NEAT) Reconfiguration to Enable Altitude Testing of Megawatt-Scale Electric Machines

Joseph M. Haglage[1]
NASA Glenn Research Center, Cleveland, OH, 44135, USA

Thomas W. Brown[2]
GE Aviation, Cincinnati, OH, 45215, USA

The NASA Electric Aircraft Testbed (NEAT) has been developed over the past four years in order to provide a testbed that enables end-to-end testing of multiple technologies that are required for the development of a hybrid-electric aircraft. NEAT has been designed to be reconfigurable, so that the facility can be used to test different technologies in appropriate ways. The testbed has recently been reconfigured from a powertrain test, to a megawatt-scale dynamometer inside of an altitude chamber. This configuration enables full-power testing of megawatt-scale components and systems under simulated altitude conditions. This paper discusses the reconfiguration design of NEAT, along with problems encountered and mitigations implemented during checkout testing to date.

I. Nomenclature

AC	=	Alternating Current
atm	=	Atmospheric Pressure
BLI	=	Boundary Layer Ingestion
COTS	=	Commercial Off the Shelf
DC	=	Direct Current
Id	=	D-axis Current
Iq	=	Q-axis Current
NEAT	=	NASA Electric Aircraft Testbed
STARC-ABL	=	Single-Aisle Turbo-electric Aircraft with Aft Boundary Layer Ingestion
VDC	=	Voltage, direct current
W	=	Watt

II. Introduction

The NASA Electric Aircraft Testbed (NEAT) has been developed over the past four years in order to provide a testbed that enables end-to-end testing of multiple technologies that are required for the development of a hybrid-electric aircraft. These technologies include [1]:

- High-voltage electrical bus architecture
- High-power motors/generators
- High-power inverters and rectifiers
- System communication
- System electromagnetic interference (EMI) mitigation and standards

[1] NASA Electric Aircraft Testbed Lead, Diagnostics and Electromagnetics Branch, non-member
[2] Lead Controls Engineer, Advanced Technology Organization, non-member

- System fault protection
- System thermal management

NEAT has been designed to be reconfigurable, so that the facility can be used to test these technologies in appropriate ways. The testbed has recently been reconfigured from a powertrain test, to a megawatt-scale dynamometer inside of an altitude chamber. This configuration will enable full-power testing of megawatt-scale electric machines under simulated altitude conditions. The powertrain test, a subscale, simplified powertrain for NASA's Single-Aisle, Turbo-electric Aircraft with Aft Boundary Layer Ingestion (STARC-ABL), is briefly described for the reader's familiarity in section III of this paper, but has been described by Dr. Rodger Dyson in previous papers [1,2].

III. Base Configuration (STARC-ABL)

In FY18, the NEAT facility was being used to conduct testing on a simplified full-scale powertrain that would be used on NASA's Single-Aisle Turbo-electric Aircraft with Aft Boundary Layer Ingestion (STARC-ABL). In STARC-ABL, turbine engines are used to drive two electric generators, one under each wing. The power generated is then routed to a fan at the tail of the aircraft, which provides additional thrust and decreases drag via boundary layer ingestion [1].

At NEAT, this configuration was built using AC-DC power supplies, and COTS electric motors and inverters. The power supplies are used to drive machines that act as turbines, which in turn drive machines that act as generator on the wings. The power generated on the wings is then routed to the rear of the facility, to motors that simulate the boundary layer ingesting (BLI) fan. Figure 1 shows a simplified one-line diagram of the STARC-ABL electrical configuration built at NEAT.

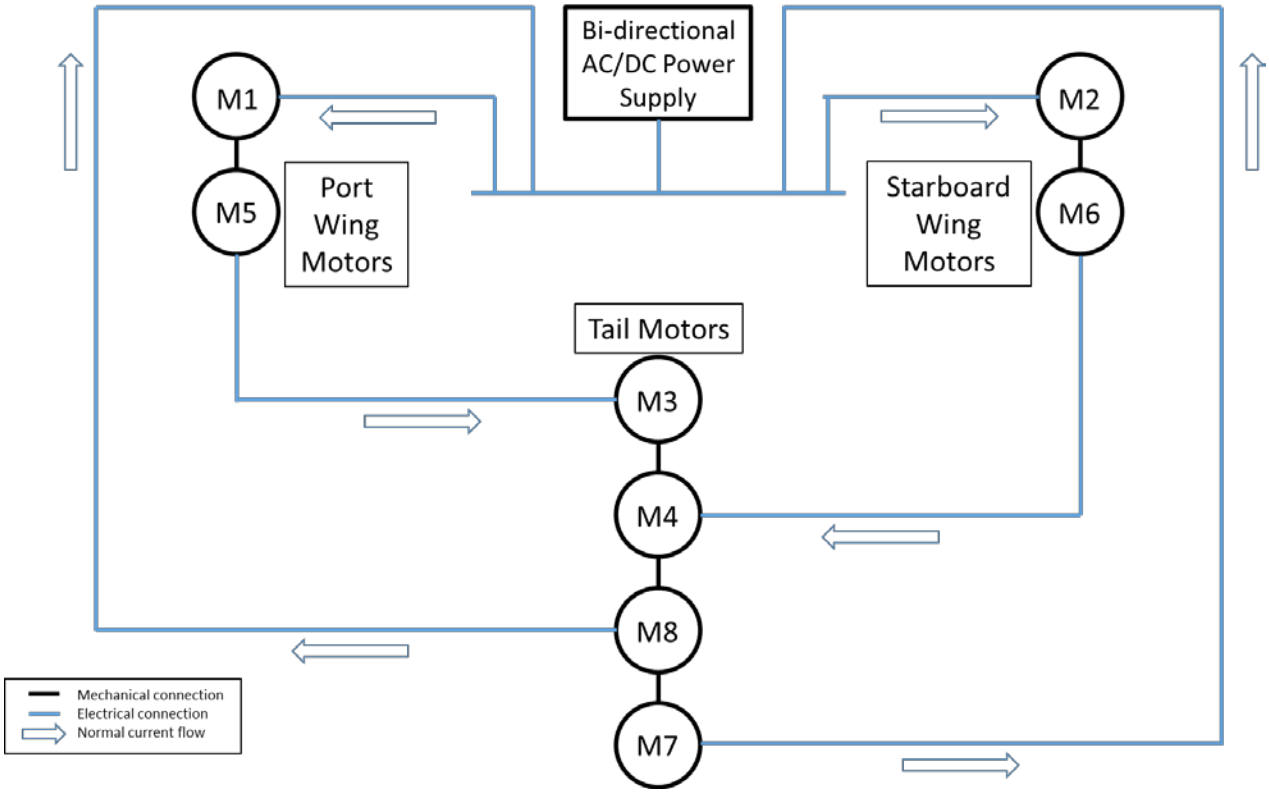

Fig. 1: Simplified 500kW STARC-ABL Configuration

Each of the COTS motors is rated for 250kW, but they can be connected on the same shaft in order to create a higher power system. In Fig 1, motors M1 and M2 represent the aircraft gas turbines, motors M5 and M6 represent generators connected to the turbine shafts, M3 and M4 represent a 500kW electric motor at the tail of the aircraft, and

M7 and M8 represent a BLI fan being driven by that motor. All STARC-ABL testing was done under sea level conditions.

IV. Reconfiguration

As part of the long-term plan for electrified propulsion technology maturation, it is anticipated that electric machines will continue to improve in both power density and efficiency, and this is a major driver for establishing feasibility for electrified propulsion in the transport class. NASA investments to date have sought machine advancements capable of achieving 13 kW/kg and >96% efficiency in order to provide a net benefit in terms of fuel burn in a turboelectric concept [3]. Performance must be met while also assuring that the machines are capable of operating in altitude conditions, which is a particular concern for solutions relying upon high voltages (>270V) as a means for weight and volume reductions. At altitude, higher voltage systems are subject to issues such as partial discharge, and therefore it will be necessary to test for safety as well as performance as the designs mature.

In order to meet the requirement of testing a megawatt-scale electric machine under altitude conditions, the NEAT facility needed to undergo a reconfiguration. Existing equipment that was being used for STARC-ABL testing needed to be configured such that a megawatt load could be supplied to an electric machine, and that the resulting energy could be dissipated safely. In order to accomplish this quickly, the Tail Motor string from the STARC-ABL design described in Section III was repurposed. These four motors were kept on a common shaft, and were then mechanically connected to the test article.

A. Original Design

1. Electrical System

In order to create an electric machine capable of providing a 1MW load, four of the COTS 250kW motors were connected on the same shaft to create a single 1MW dynamometer. An electrical system needed to be designed that could initially provide power to the four motors in order to begin spinning the system, and then sink the electrical power generated when the test article began producing power. A simplified schematic of the original electrical design of the system is shown in Fig 2. The four COTS motors are shown on the right-hand side of the figure.

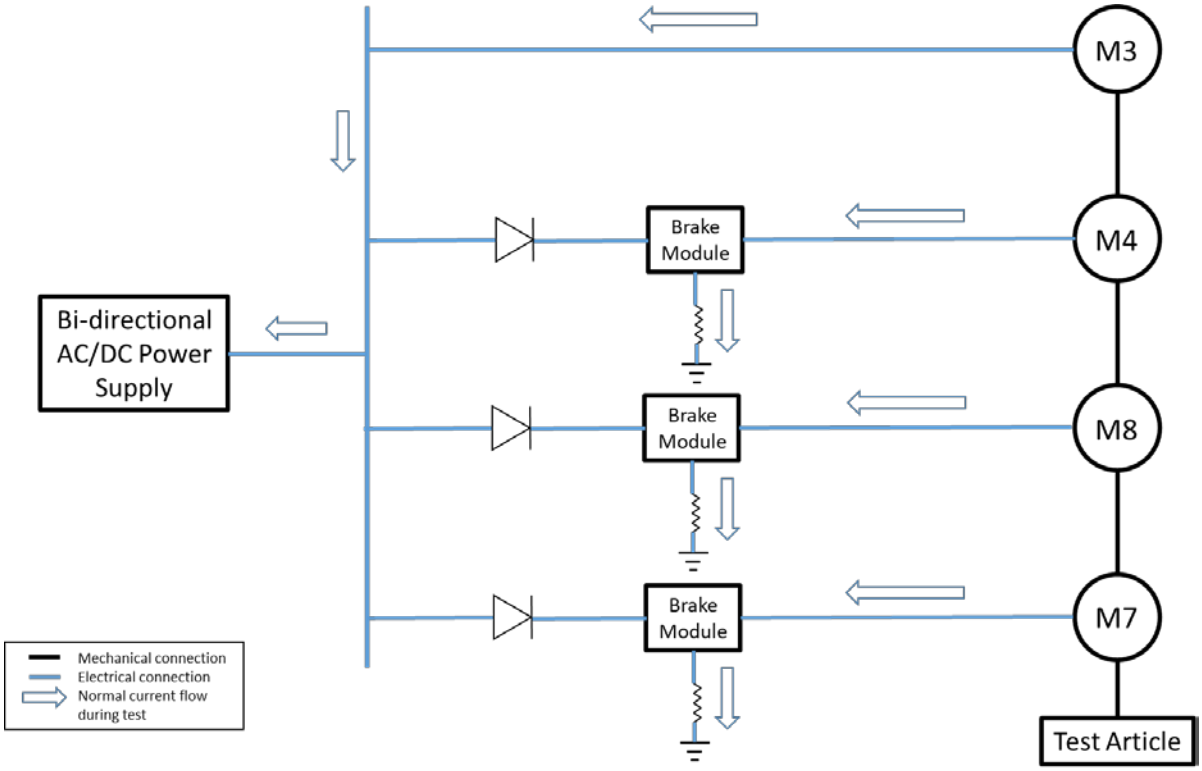

Fig. 2: Original Electrical Design Concept for 1MW Motor Test

The bi-directional power supply was rated for 275kW. Therefore, in order to keep from exceeding that rating, only one of the four 250kW motors ("M3" in Fig 2) was connected directly to the power supply. Each of the other three motors were connected to the power supplies via a blocking diode and a COTS brake module. This configuration effectively created four separate electrical buses when the dynamometer was generating power. As the motors started generating power, current from the M3 bus flowed back through the bi-directional power supply and onto the grid. On the M4, M7, and M8 buses, current was blocked by the diode, and the voltage on these buses would rise. When the voltage surpassed a user-defined voltage set point in the brake module, the brake module would switch a resistive load on and off of the DC bus in order to control the voltage. This design had the effect of enabling the COTS motors to spin up the test article with no load, and then dissipate power once the dynamometer began generating power. However, the switching action of the brake modules did contribute to DC current ripple that was discovered during system checkout. This DC current ripple is discussed further in parts B and C of this Section.

2. Mechanical System

In order to protect the COTS equipment from the altitude environment, the four motors, four inverters, and all associated communications, control, and data collection equipment were installed on a 19' long table and encased in a metal shroud. The shroud was designed to withstand a pressure difference of 14 psi. The table and shroud were installed within the altitude chamber, and the shroud was vented to the high bay area. This installation has the effect of keeping the inside of the shroud pressurized to 1 atm while the rest of the chamber is pumped down to simulate altitude conditions. Fig 3 shows the motors, inverters, cabling, and control and data acquisition boxes installed on the table without the shroud lid installed. Fig 4 shows the table with the shroud lid in place.

Fig. 3: Dynamometer Table without Shroud Lid Installed

Fig. 4: Dynamometer Table with Shroud Lid Installed

The orange tubes leading into the shroud shown in Fig 4 lead to the high bay area of the facility and serve two purposes. As mentioned above, they keep all equipment installed underneath the shroud pressurized to 1atm, while the rest of the chamber is pumped down to a simulated altitude. They also create a convenient path for power and instrumentation cabling. The high power cables run through two dedicated tubes, and instrumentation and communication cables run through the other two.

B. Problems Encountered

During checkout testing of the 1MW dynamometer system, a large ripple current was discovered on the DC power bus. A screen capture of an oscilloscope monitoring the current and voltage of two of the motors is shown in Fig 5.

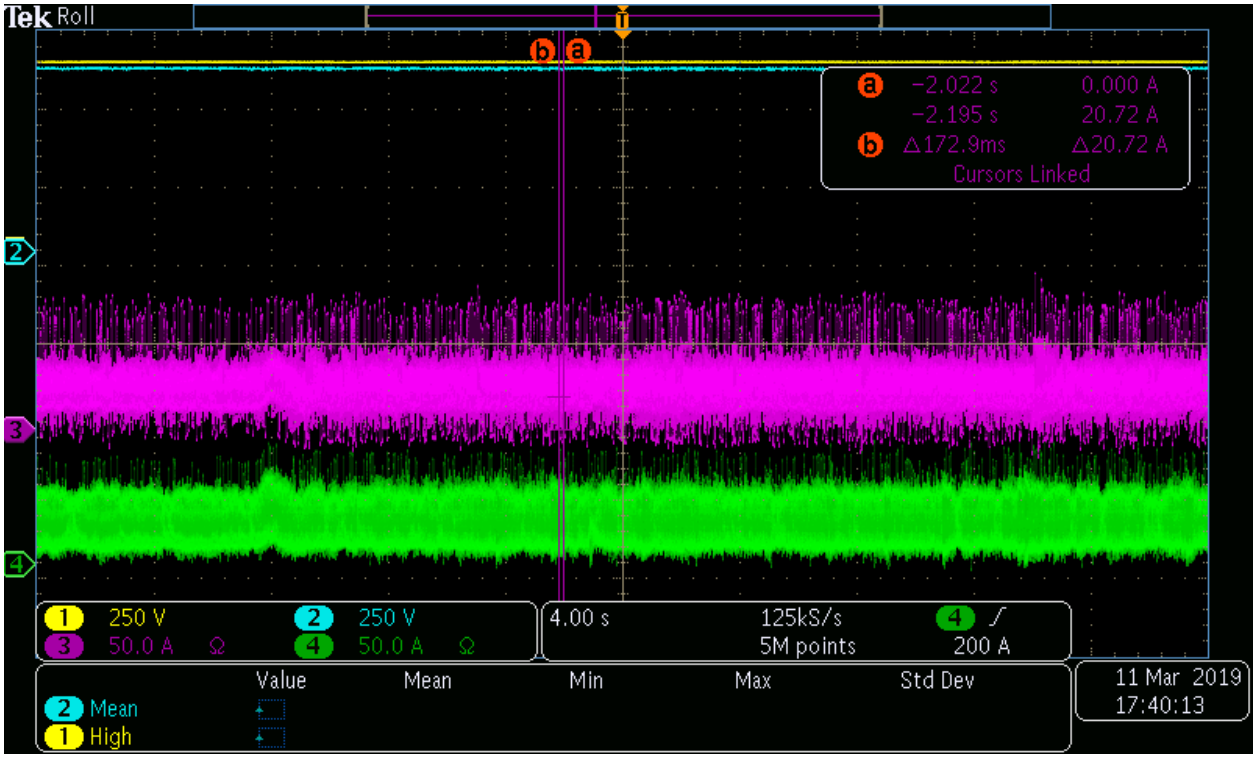

Fig. 5: Oscilloscope Capture of DC Current Ripple

On channel 3 of the oscilloscope (shown in purple), a peak-to-peak ripple of approximately 90A is seen on top of a DC current of approximately 40A. This high ripple often caused the DC power bus to become unstable, resulting in the tripping off of either the power supplies or the inverters. Fig 6 shows an example of the current ripple causing a trip event, signified by the sudden drop to zero current shown on channels 3 and 4 (shown in purple and green, respectively), and the slow decrease in voltage (shown in blue and yellow) due to the bleed-down of capacitance on the bus. Fig 7 shows a further zoomed-in version of a similar, though separate, trip event.

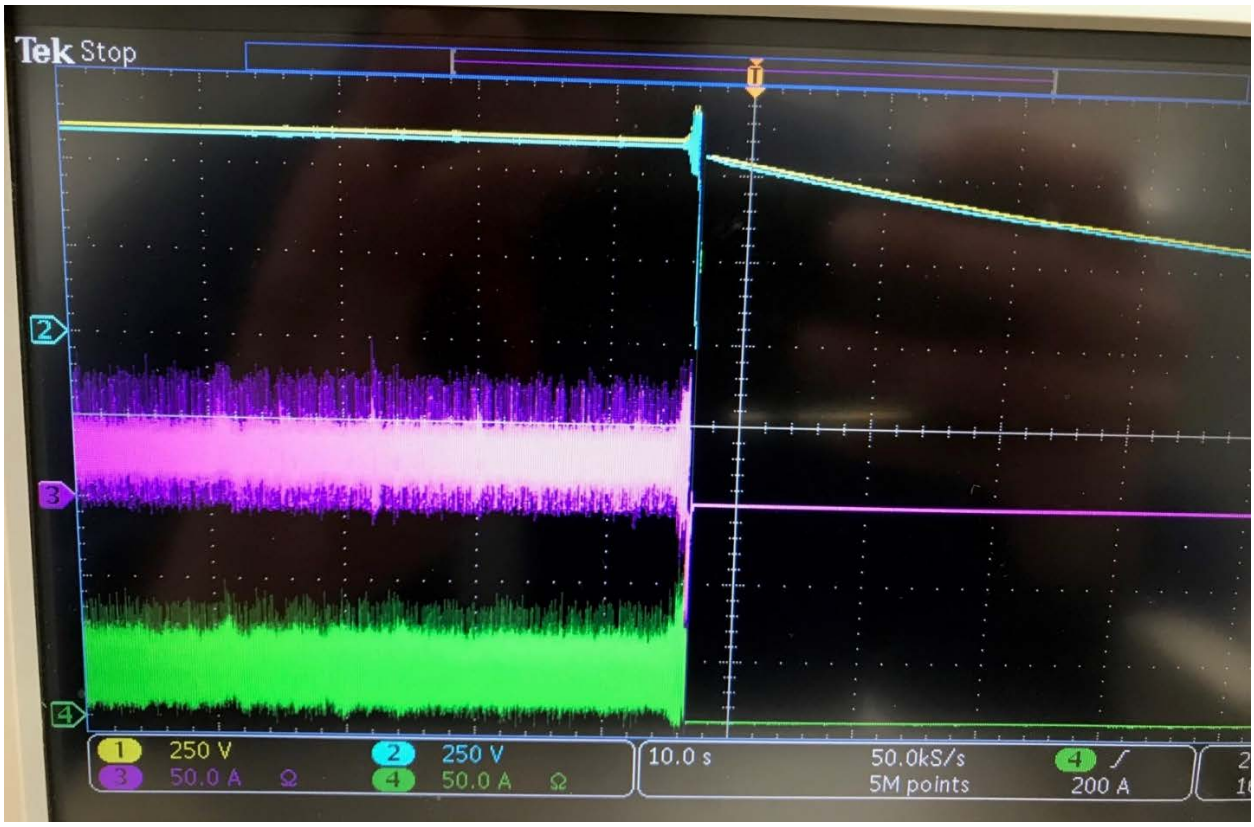

Fig. 6: Current and Voltage Traces during a Trip Event Due to Ripple

Fig. 7: Current Waveform Immediately Preceding a Trip Event Due to Ripple

As a first means of troubleshooting, a capacitor bank was installed across the terminals of the power supplies to dampen any ripple that they might put onto the bus. Bus ripple was unchanged with the capacitor bank installed, thus eliminating the power supplies as the source of ripple.

Next, analysis of the dynamometer motor flux map and inverter telemetry was performed to identify any ripple that these components were causing on the DC bus. A negative d-axis AC inverter current was observed at high dynamometer speeds, indicative of the inverters entering flux weakening mode. This negative d-axis AC inverter current was not observed at lower dynamometer speeds. Fig 8 shows a generic flux map for a permanent-magnet electric machine (the same architecture utilized by the dynamometer motor/generators) at nominal voltage and low speed. The green arrow represents the current vector at this low speed operating point, where flux weakening mode was not required because the low speed precluded limitation by the voltage constraint.

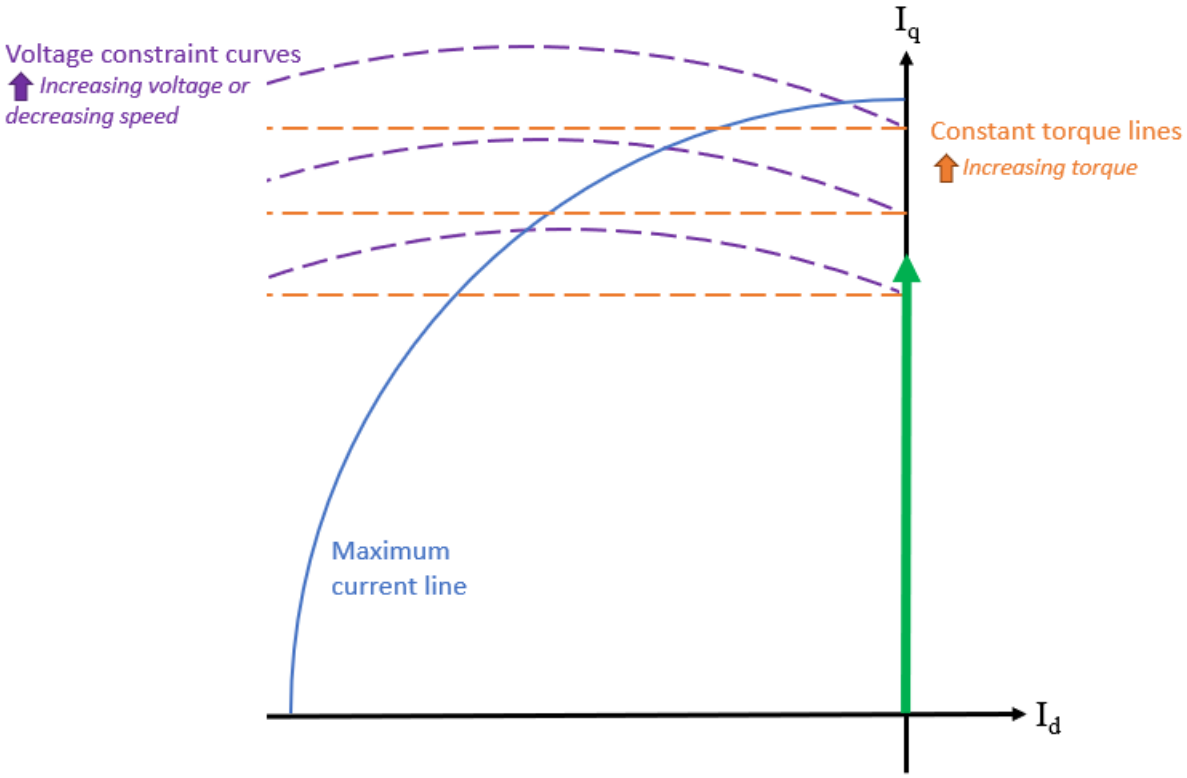

Fig. 8: Id vs. Iq Diagram at Low Speed Point

At high speed, the dynamometer needed to operate in flux weakening mode to achieve the same torque. Since voltage remained constant while speed increased, the voltage constraint moved closer to the I_d axis. This voltage constraint required a negative I_d component to achieve the desired torque. The green line in Fig 9 represents the current vector at this high-speed condition, while the grey line represents the path to that point. This entrance into flux weakening mode occurred at a torque that was lower than expected, which could indicate a controls or tuning instability that contributed to the ripple on the DC bus.

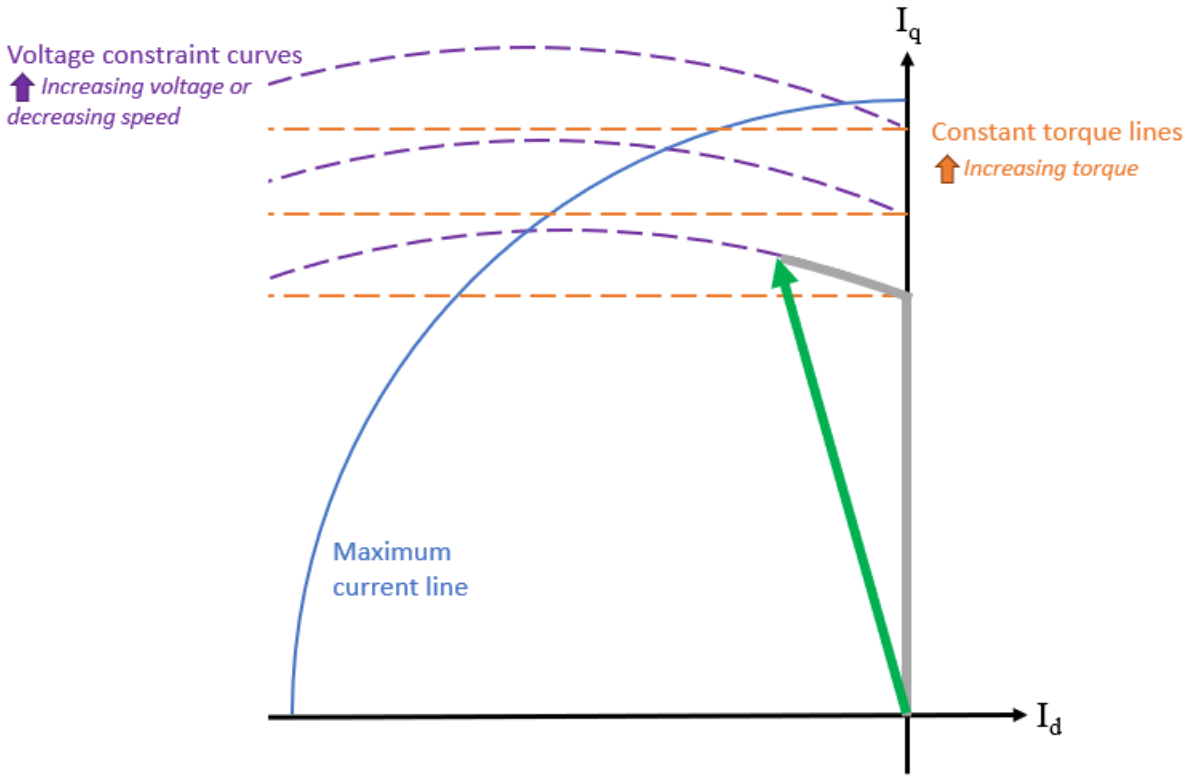

Figure 9: Id vs. Id Diagram at High Speed in Flux Weakening

C. Mitigations Implemented

In light of the problems caused by DC current ripple, two main mitigations were implemented: the operating voltage was raised in order to operate the motors outside of their field-weakening region, and the brake modules were removed in favor of a passive load resistance that did not require constant switching.

Analysis of the dynamometer motor flux map indicated that these machines were operating in their flux weakening region due to the nominal DC bus voltage of 600VDC. In the electrical system's design phase, the maximum nominal DC bus voltage was constrained by the voltage set point of the brake modules. By replacing the brake modules with a resistive load, the nominal DC bus voltage could be increased to 700VDC, moving dynamometer motor operation out of the flux weakening region. This addressed both potential causes of DC bus instability described previously. This is illustrated in Fig 8 below, where the green arrow illustrates the current vector at high speed and an increased voltage. The elevated voltage constraint precludes operation in flux weakening mode throughout the dynamometer operating range, which was observed to decrease bus current oscillations to an acceptable level.

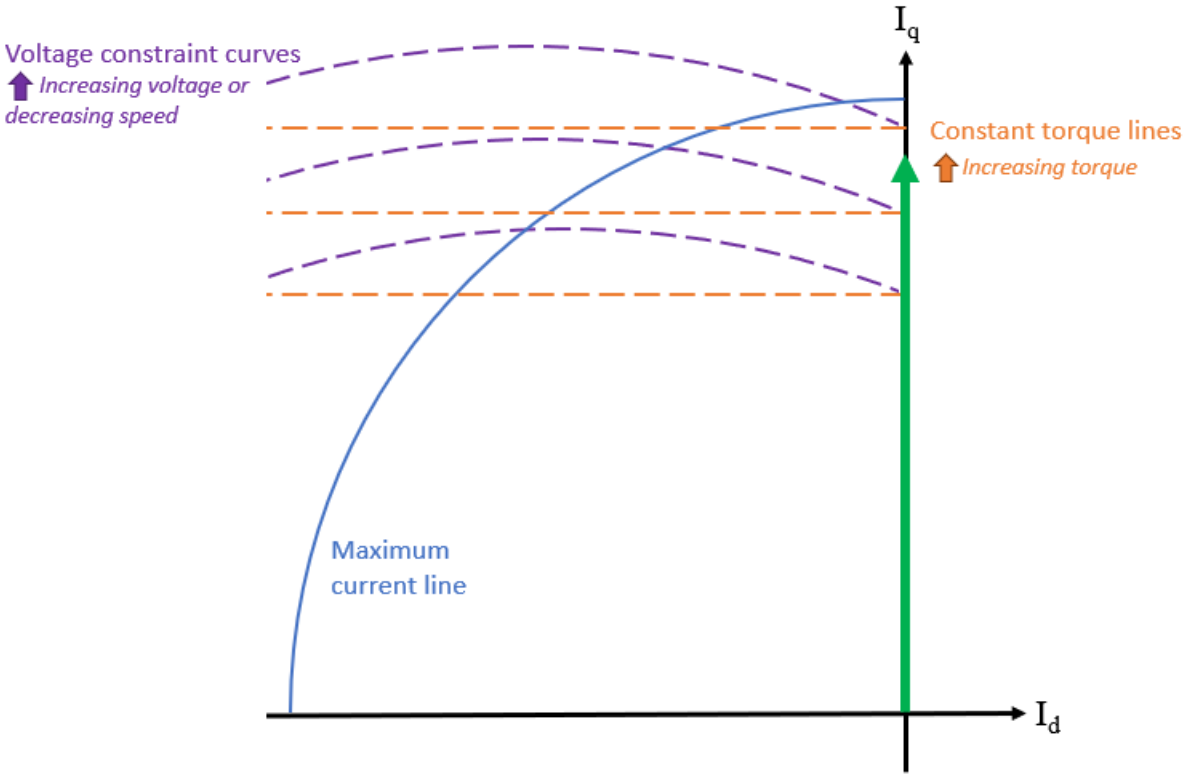

Figure 10: Iq vs. Id Diagram at High Speed with Increased Bus Voltage

The resistive load implemented was a passive system requiring external control of its load steps. Using a passive system eliminated the portion of DC bus ripple caused by the fast-switching solution of the brake modules. To accomplish control of this passive system, a supervisory controller monitored system telemetry and automatically applied or removed resistive load steps as necessary to keep the power supplies within rated operational parameters.

A simplified schematic of the final configuration of the electrical system used during testing is shown in Fig 11.

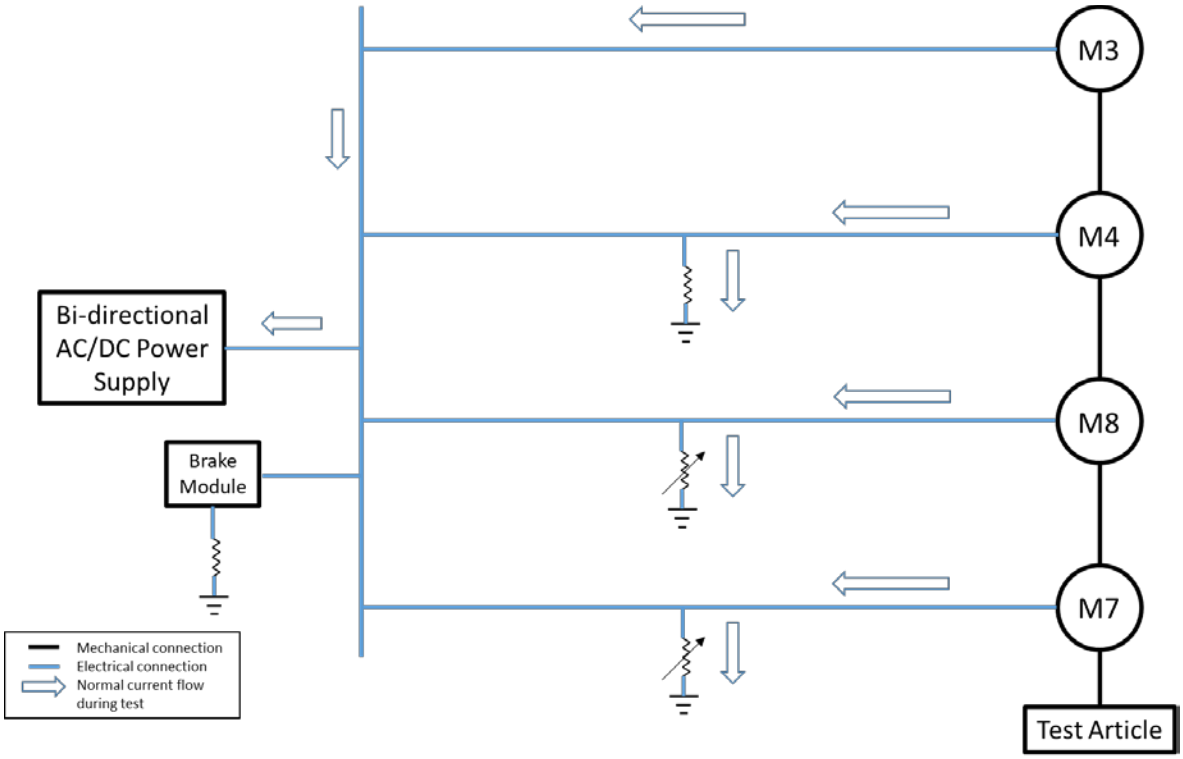

Fig. 11: Final Configuration of 1MW Machine Altitude Test

As shown in Fig 11, the removal of the three blocking diodes had the effect of a single common bus for all four motors during regeneration. A single, 82kW resistive load was permanently connected to M4, and the two adjustable load banks (each rated at 340kW at 700VDC), are represented by the two potentiometers connected to M8 and M7. These three resistive loads, in combination with the 275kW sinking capability of the bidirectional power supply, were enough to safely dissipate all of the power available from the 1MW dynamometer system. It should be noted that because of the nature of the common bus, the physical locations of these loads was of little importance. It should also be noted that a brake module was kept installed in the system as a safety precaution. It would have only been used in the event of a load failure that caused a voltage rise on the bus, and was not used in normal operation.

All active components on the DC bus retained their internal undervoltage and overvoltage protection, providing safety against faulty closing or opening of resistive load steps. After the system reconfiguration and implementation of the automatically adjustable resistive load system, the previously observed ripple on the DC bus was reduced to the point of enabling continuous, stable operation of the dynamometer system. This enabled exercising of the unit-under-test across its full operating envelope.

V. Conclusion

The facility reconfiguration described above allowed NEAT to successfully complete the test of a megawatt-scale electric machine under altitude conditions. Although the mitigations that were implemented did reduce the DC current ripple to the point of being able to successfully operate continuously, a significant ripple was still seen on the bus during test. Further research and testing is required to reduce the peak-to-peak current as much as possible.

NEAT has proven to be a very powerful tool for testing hybrid-electric aircraft technologies. The reconfigurable nature of the facility allows for both high-power single component testing, as well as full system testing at the same facility. As NEAT continues to mature, the transitions between tests will become smoother, and downtime between tests will be minimized.

Acknowledgments

The reconfiguration of the NASA Electric Aircraft Testbed was funded by the Advanced Air Transport Technology project/Hybrid Gas Electric Propulsion subproject, with support from GE Aviation. The authors would like to thank Ralph Jansen, Paul Gemin, Di Pan, Tim Dever, and Pete Kascak, along with the VPL staff and TFOME staff.

References

[1] Dyson, R., "NASA Electric Aircraft Testbed (NEAT) "Single-Aisle Transport Air Vehicle Hybrid Electric Tail-Cone Thruster Powertrain Configuration and Test Results," AIAA Paper 2018-5004, July 2018.
[2] Dyson, R., "NASA Electric Aircraft Testbed (NEAT) Development Plan – Design, Fabrication, Installation," NASA TM-2016-219085, 2016.
[3] Duffy, K., and Jansen, R., "Turboelectric and Hybrid Electric Aircraft Drive Key Performance Parameters," AIAA 2018-5023, July, 2018.